JOURNAL OF SOLID STATE CHEMISTRY 93, 154–162 (1991)

EXAFS and XANES Studies of the TmCrAl Garnet Crystallization Process

HEIKE NIEMANN, A. TORKLER, M. A. DENECKE, AND W. GUNSSER*

Institute of Physical Chemistry, University of Hamburg, Bundesstrasse 45, D-2000 Hamburg 13, Germany

AND WILHELM NIEMANN†

Haldor Topsøe Research Laboratories, Nymøllevej 55, DK-2800 Lyngby, Denmark

Received August 23, 1990; in revised form March 8, 1991

The transformation of amorphous, coprecipitated Tm(III), Al (III), and Cr(III) oxyhydroxides to polycrystalline $\{Tm_3\}[Cr_2](Al_3)O_{12}$ garnet (TmCrAlG) was monitored at various annealing temperatures by differential thermal analysis (DTA), X-ray diffraction (XRD), and X-ray absorption spectroscopy (XAS). Extended X-ray absorption fine structures (EXAFS) were analyzed to determine the metal–oxygen bond distances and the number of nearest oxygen neighbors as a function of the annealing temperature. Information concerning the scattering geometry around the 3*d* transition metals was derived from X-ray absorption near-edge structure (XANES) measurements through quantitative analysis of the ($1s \rightarrow 3d$) prepeak at the K-edges. We were able to show that Cr(III) enters exclusively octahedral sites in the crystalline garnet.

Introduction

The short-range order (sro) and magnetic properties of X-ray diffraction (XRD) amorphous rare-earth transition metal garnets have been investigated by several authors (*1–7*). Differences in magnetic properties seem to result from variations in the local cation environment (*8*), which is significantly influenced by the preparation conditions (e.g., splash-cooling, sputtering, twin-roller quenching, and wet chemical methods). In the present work we apply a novel and sensitive method (XAS = X-ray absorption spectroscopy) for determining cation coordination numbers and bond distances during the calcination process of amorphous thulium chromium aluminum oxyhydroxides $(3Tm/2Cr/3Al/xO)$[1] to $\{Tm_3\}[Cr_2](Al_3)O_{12}$ c-garnet (TmCrAlG). For comparative purposes the crystallization of thulium iron oxyhydroxides $(3Tm/5Fe/xO)$[1] to $\{Tm_3\}[Fe_2](Fe_3)O_{12}$ c-garnet (TmIG) was studied as well. XAS is es-

* To whom correspondence should be addressed.

† Present address: Philips Research Laboratories Vogt-Kölln-Straße 30, D-2000 Hamburg 54, Germany.

[1] The formulae $3Tm/5Fe/xO$ and $3Tm/2Cr/3Al/xO$ refer to cation stoichiometry only, with no structural implications.

0022-4596/91 $3.00

pecially suited for studying the sro of the individual cations due to its unique elemental selectivity.

In c-TmIG octahedral as well as tetrahedral sites are occupied by Fe(III) (*8*). Substitution of Fe(III) by Cr(III) and Al(III) leads to the 3Tm/2Cr/3Al/xO system. Cr(III) was chosen because it is a candidate which may, despite its having a smaller ionic radius than Fe(III), exclusively enter the octahedral sites and which also can be prepared as an oxyhydroxide. Al(III) was chosen for the substitution of the tetrahedral site.

Freshly precipitated oxyhydroxides were XRD amorphous. Continuous annealing of the precipitated samples was monitored with differential thermal analysis (DTA) revealing an initial dehydroxylation, followed by a diffusion process and the final crystallization. Samples of amorphous precursors were annealed to temperatures below the crystallization temperature, T_c, and their sro was investigated using XAS. Extended X-ray absorption fine structure (EXAFS) data provide information concerning backscattering species, distance (R), and number of nearest neighbors (N). The X-ray absorption near edge structures (XANES) contains additional information on geometry, valence, and bond angles. In this paper, particular attention is given to the exploitation of the ($1s \rightarrow 3d$) prepeak for obtaining structural information.

Experimental

Samples were prepared by coprecipitating the oxyhydroxides in the stoichiometric cation ratio of garnet. The precipitation was performed in an ultrasonic field (24 kHz) to prevent inhomogeneous nucleation. High miscibility and rapid precipitation of the hydroxides prevents crystallization of the precursors. After washing, filtering, and drying, the hydroxides were annealed up to temperatures between 60 and 1200°C (heating rate: 5°C/min) and subsequently cooled (cooling rate: 20°C/min). For a more detailed description of the preparation see Refs. (*9*, *10*).

EXAFS and XANES measurements were carried out at the EXAFS II beamline of the Hamburger Synchrotronstrahlungslabor HASYLAB (*11*) using a Si (111) double crystal monochromator (2.5 keV $\leq E \leq$ 14 keV). The powder samples ($\mu * d \sim 2$) were prepared on Kapton foils. The experiments were performed at 10 K.

Results and Discussion

DTA Measurements

DTA diagrams for continuously annealed oxyhydroxides of the 3Tm/5Fe/xO and 3Tm/2Cr/3Al/xO systems are shown in Fig. 1. Up to ~500°C the calcination process is dominated by an endothermic decomposition of the oxyhydroxides (*12*) accompanied by a sample weight loss. Upon further annealing, the weight of the powdered samples

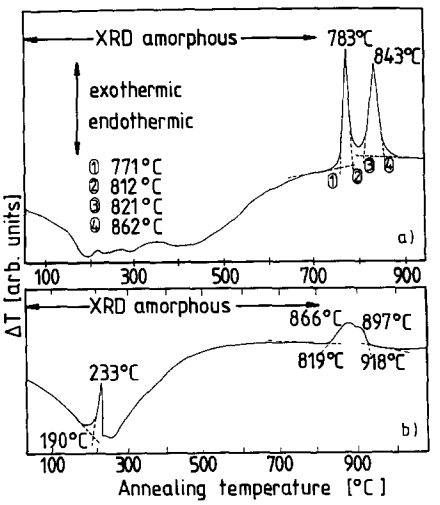

FIG. 1. DTA diagrams of the (a) 3Tm/5Fe/xO and the (b) 3Tm/2Cr/3Al/xO systems (heating rate: 5°C/min).

remains constant and the thermic energy is used to stimulate ion diffusion until T_c is reached. For both systems under investigation the crystallization process is found to be divided into two phase transitions, indicating that crystallization to garnet occurs via a metastable phase or phase mixture. The maxima of the two exothermic DTA peaks in the 3Tm/5Fe/xO and the 3Tm/2Cr/3Al/xO systems are separated by ~60°C and ~30°C, respectively. Reznitskii *et al.* (*13*) found a similar behavior by annealing a stoichiometric mixture of yttrium (or erbium) and iron hydroxides to YIG (or ErIG) and identified the metastable phase at the first phase transition temperature as a mixture of Y_2O_3 (or Er_2O_3), garnet, and α-Fe_2O_3. The 3Tm/2Cr/3Al/xO system exhibits an additional exothermic peak at 190°C. Chromium K-edge XANES results show that this corresponds to the oxidation of some Cr(III) to Cr(VI).

XRD Results

The annealed sample mixtures of both systems were XRD amorphous up to temperatures approaching T_c. The 3Tm/5Fe/xO system crystallizes to TmIG via a metastable phase mixture of Tm_2O_3 and α-Fe_2O_3. At 790°C α-Fe_2O_3 and Tm_2O_3 have already partly reacted to TmIG, as indicated by a weak 420 reflection at $2\vartheta = 32.6°$ (Cu$K\alpha$). At the applied slow cooling rate of 20°C/min, we were unable to isolate the metastable phase for the 3Tm/2Cr/3Al/xO system. We will demonstrate below that this may be due to the kinetics of the phase transition.

EXAFS Results

EXAFS analyses were performed based on standard plane wave theory (*14*) using experimentally determined backscattering amplitudes and total phases. This resulted in absolute errors of $\Delta R = \pm 0.02$ Å for interatomic distances and $\Delta N = \pm 1$ for coordination numbers.

Thulium L_{III}-edge EXAFS

Figures 2a–2b depict the EXAFS oscillations of the Tm L_{III}-edge in the 3Tm/2Cr/3Al/xO system, as well as the corresponding Fourier transforms (FTs). Mean Tm–O bond lengths and mean coordination numbers (Fig. 3a,b) were obtained from a single shell fit of the Fourier-filtered EXAFS of this and the 3Tm/5Fe/xO system. The experimental total phase and backscattering amplitude from c-TmIG were used in the fit procedure. Due to the coexistence of several Tm–O distances in the garnet, the demodulation procedure described in (*15*) was used to obtain single shell quantities. The mean coordination number and mean Tm–O distance of the amorphous TmOOH obtained are nearly identical to the data for the crystalline thulium oxyhydroxide (*16*). Both these quantities were found to decrease with increasing temperature in the amorphous garnet. At temperatures slightly below T_c the parameters for the amorphous system show a maximum deviation from the crystalline data. This could explain why the crystallization does not occur in one step but via a metastable oxide mixture of Tm_2O_3 and α-Fe_2O_3. In the 3Tm/2Cr/3Al/xO system the difference between the bond lengths of Tm–O in the amorphous state and in the crystalline state is less pronounced. The crystallization to TmCrAlG is much faster and a metastable phase mixture was not isolable under the applied conditions.

Iron K-edge EXAFS

A structure similar to crystalline α-FeOOH (*17*) was found for the precipitated iron oxyhydroxide (T = 60°C). This structure persisted up to ~460°C. α-Fe_2O_3, a constituent of the metastable phase mixture, was detected in the Fe K-edge EXAFS data of the sample annealed up to 790°C. At temperatures higher than this, the back transforms (BTs) of the Fe–O shell could be fitted

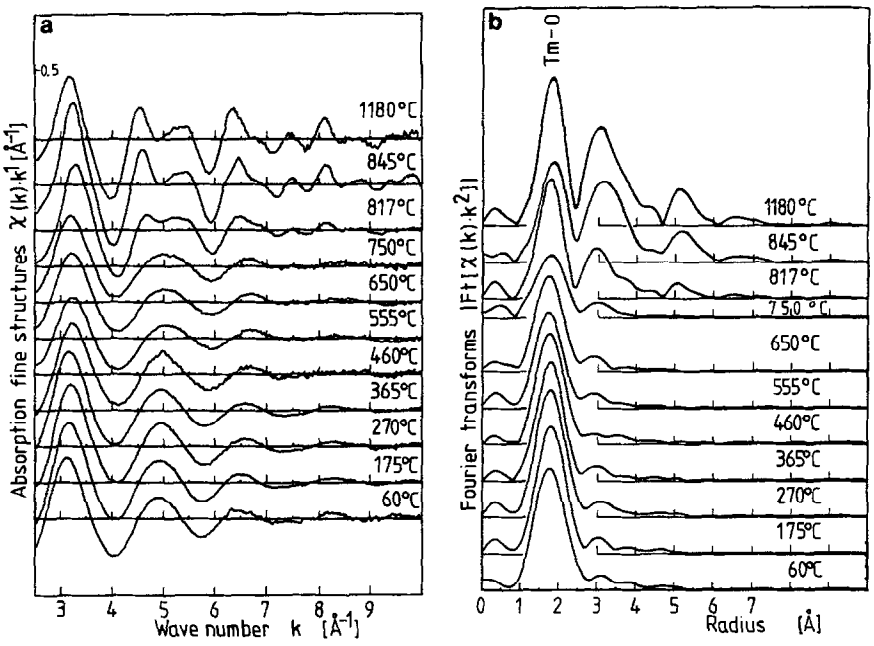

FIG. 2. (a) Tm L_{III}-edge EXAFS for 3Tm/2Cr/3Al/xO samples annealed at temperatures indicated; (b) Fourier transforms of (a) (Kaiser–Bessel window, transformation region between 2.0 and 9.0 Å^{-1}, k^2 weighting).

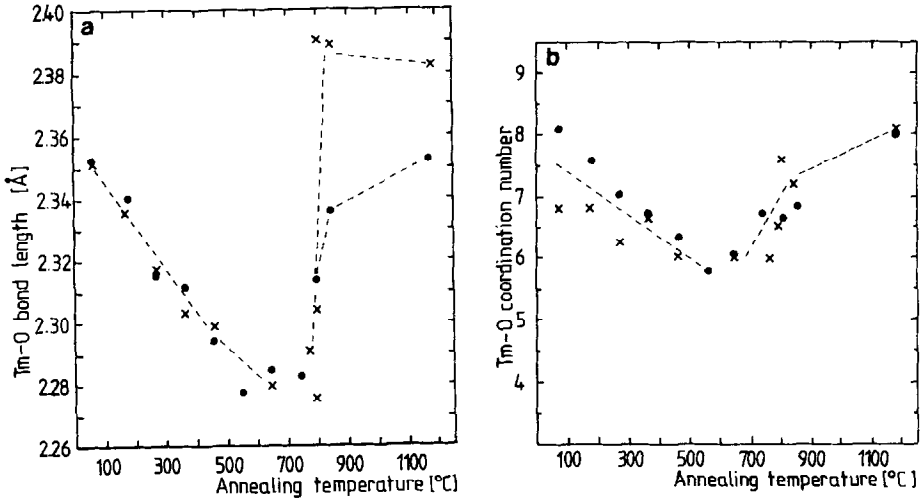

FIG. 3. Results of the single-shell fit at the Tm L_{III}-edge; (a) mean Tm–O bond length as a function of the annealing temperature; (b) mean EXAFS coordination number of the scattering pair Tm/O as a function of the annealing temperature (×, 3Tm/5Fe/xO, ●, 3Tm/2Cr/3Al/xO).

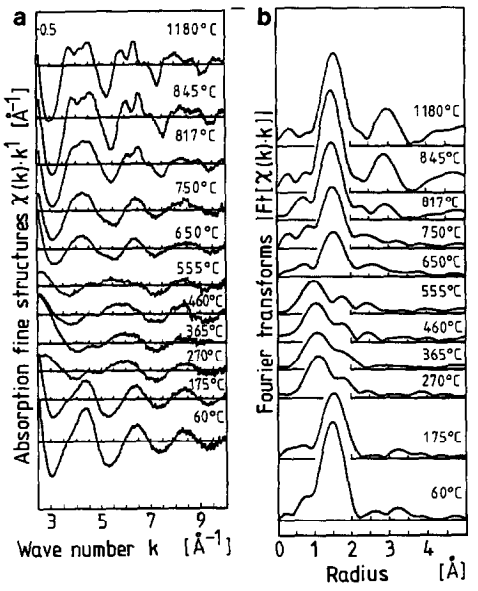

FIG. 4. (a) Cr K-edge, EXAFS for 3Tm/2Cr/3Al/xO samples annealed at temperatures indicated. (b) Fourier transforms of 4(a) (Gaussian window, transformation region between 2.0 and 9.0 Å^{-1}, k^1 weighting).

as two subshells (corresponding to tretrahedral and octahedral sites) using Fe–O scattering and phase functions again from c-TmIG.

Cr K-edge EXAFS

Figure 4 shows the EXAFS and their FTs from Cr K-edge absorption measurements of the 3Tm/2Cr/3Al/xO system. The change in the EXAFS at 270°C compared to 175°C shows that the DTA peak detected at 190°C corresponds to a structural change. Associated with this is a change in the chromium valence from (III) to (VI), evident from the shift of the absorption edge to higher energies (Fig. 7). The energy shift of the Cr K-edge is small (1.5 eV) compared to the edge shift between Cr_2O_3 and CrO_3 (4.1 eV), indicative of an incomplete oxidation of Cr(III). In the temperature region between 270 and 555°C destructive interference of several subshells leads to very small EXAFS amplitudes. An EXAFS simulation using a linear combination of the nearest neighbor Cr–O parameters (N, R) of Cr_2O_3 (*18*) and CrO_3 (*19*) and the total phase and backscattering amplitude for the scattering pair Fe/O from TmIG was used to estimate the amounts of Cr(III) and Cr(VI) present at various annealing temperatures. At 555°C it was found that the relative amounts of Cr(III) to Cr(VI) oxides were 35% : 65%. At the following temperature (650°C) the simulation resulted in a ratio of 60% : 40%. The first chromium coordination shell undergoes reorganization between the temperatures of 555 and 845°C. c-TmCrAlG is finally formed at 890°C.

The BTs of the Cr–O coordination have been fitted using either a single-shell fit (for samples annealed at 60, 845, and 1180°C) or a three-shell fit (for samples annealed up to temperatures between 175 and 555°C). The EXAFS parameters N and R so determined are presented in Figs. 5a and 5b. The results demonstrate that at the beginning of the annealing process two-thirds of Cr-oxygen polyhedra undergo a change in their geometry accompanied by an oxidation of Cr(III) to Cr(VI), resulting in a sharp decrease in Cr–O bond lengths. The reconstruction of tetrahedrally coordinated Cr(VI) to octahedrally coordinated Cr(III) already takes place about 200°C below the crystallization of TmCrAlG, meaning that the crystallization of TmCrAlG may proceed faster than in TmIG. This could explain why the metastable phase was not isolated: the cooling rate (20°C/min) used was not sufficient for isolating the metastable oxides in this system.

XANES

All EXAFS results of the transition metals (Cr, Fe) have been supported through the analysis of their XANES spectra shown in Figs. 6 and 7. The edge jumps of the spectra have all been normalized to unity. The XANES region below the ionization

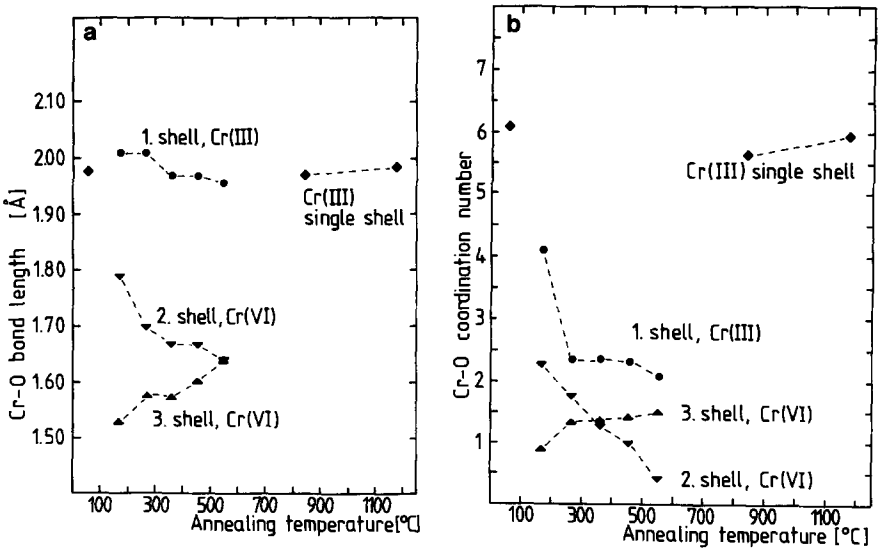

FIG. 5. Results of the Cr K-edge EXAFS; (a) Cr–O bond lengths of the 3Tm/2Cr/3Al/xO system as a function of the annealing temperature; (b) EXAFS coordination numbers of the scattering pair Cr/O as a function of the annealing temperature.

threshold involves transitions of the 1s electron into empty bound states. A significant transition is the (1$s \rightarrow$ 3d) transition, which formally is a quadrupole transition ($\Delta l = \pm 2$) with a weak transition probability in octahedrally coordinated 3d transition metal compounds but a high transition probability in tetrahedrally coordinated 3d metal (*19, 20*). In K-edge XANES spectra of 3d transition metal cations with an ideal octahedral sro of oxygen neighbors, there is no prepeak (*21–23*). Small distortions in the octahedra lead to small prepeak intensities. Tetrahedrally coordinated cations show a much

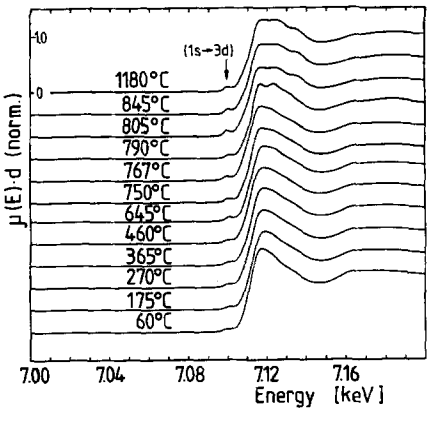

FIG. 6. XANES of 3Tm/5Fe/xO measured at the Fe K-edge, annealed at temperatures indicated.

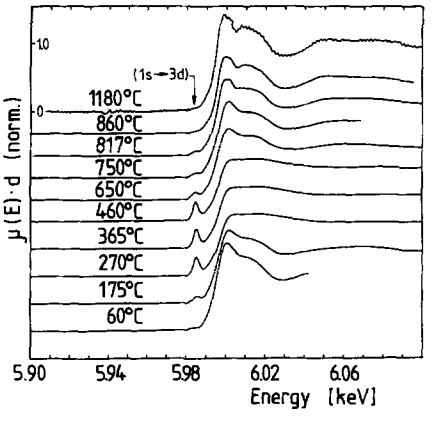

FIG. 7. XANES of 3Tm/2Cr/3Al/xO measured at the Cr K-edge, annealed at temperatures indicated.

larger ($1s \rightarrow 3d$) transition intensity (*24*) due to the greater $2p$–$3d$ orbital interaction. In this case, the increasing p-character of the $3d$ MOs results in an increasing amount of dipole character in the ($1s \rightarrow 3d$) transition. The intensity of the ($1s \rightarrow 3d$) prepeak in tetrahedrally coordinated cations is also dependent upon the number of available empty $3e$ and $2t_2$ MOs. The transition probability increases from Fe(III) to Cr(III) and finally to Cr(VI). The area of the prepeaks of the Fe and the Cr K-edge were determined as a function of the annealing temperature. The shape of the prepeak was approximated by a symmetrical Gaussian function.

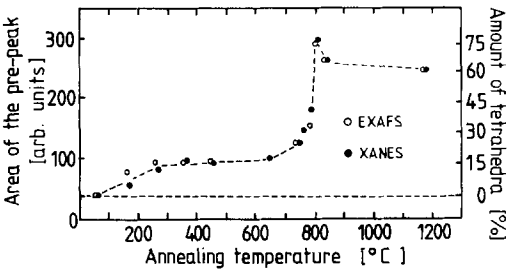

FIG. 8. Comparison between the percentage tetrahedrally coordinated Fe calculated from EXAFS coordination numbers of Fe(III)/O scattering pairs have typical tetrahedral bond distances and the area of the prepeak of the Fe K-edge.

Fe K-edge XANES

The Fe K-edge XANES of the 3Tm/5Fe/xO system annealed at T = 60°C shows a small but definite prepeak. This could be the result of the intense distortion of octahedrally coordinated Fe in α-FeOOH. This area was defined as the offset for the determination of the amount of tetrahedrally coordinated Fe(III), and all prepeak areas were corrected for this area. The amount of tetrahedrally (60%) as well as of octahedrally (40%) coordinated Fe(III) in c-TmIG is well known and was used as a calibrant for calculating the amount of tetrahedrally coordinated Fe(III) in the oxyhydroxides and annealed samples. These results, together with the percentage tetrahedrally coordinated iron obtained from EXAFS coordination numbers of the Fe(III)/O scattering pairs having bond lengths typical for tetrahedrally coordinated Fe(III), are presented in Fig. 8. EXAFS and XANES results are in good agreement.

Cr K-edge XANES

No prepeak was detected in the Cr K-edge XANES of c-TmCrAlG (Fig. 7); all Cr(III) cations are octahedrally coordinated in oxygen sublattices. Cr(III) cations exclusively enter octahedral sites, thus disproving the predictions of Geller *et al.* (*26*). The prepeak of the Cr K-edge XANES for the amorphous 3Tm/2Cr/3Al/xO system (T = 60°C) can also be interpreted as being due to small distortion in the octahedral oxygen environment of Cr oxyhydroxides. This distortion, however, seems to be small and no offset correction was made. The amount of tetrahedrally coordinated Cr as determined from the prepeak area (using CrO_3 as standard) and from theEXAFS analysis is shown in Fig. 9 for the various annealing temperatures. Differences between the EXAFS and the XANES results may be due to the large uncertainties in the EXAFS data analysis because of the aforementioned small EXAFS oscillatory amplitudes in the temperature range between 270 and 460°C.

Concluding Remarks

Our results give the following picture of the structural changes during the annealing process of 3Tm/5Fe/xO and 3Tm/2Cr/3Al/xO: Following the initial dehydroxylation, diffusion processes lead to small particles of oxides at annealing temperatures close to T_c. These react spontaneously in a thermally

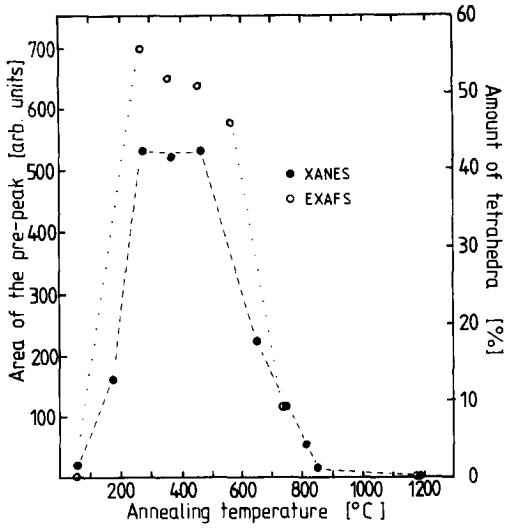

FIG. 9. Comparison between the EXAFS coordination numbers of Cr(VI)/O scattering pairs and the area of the prepeak of the Cr K-edge.

activated reaction to c-garnet. In both systems, TmOOH decomposes to Tm_2O_3, which spontaneously stabilizes to its dodecahedral coordination in c-garnet. This process involves a change in the Tm-coordination number from 8 to 6 and finally to 8. In the 3Tm/5Fe/xO system the amount of tetrahedrally coordinated Fe(III) increases slowly with increasing calcination temperature, with the majority of Fe–O polyhedra remaining octahedra. Approaching T_c, a spontaneous increase in tetrahedrally coordinated Fe is found, attaining 60% tetrahedra and 40% octahedra in c-TmIG. In comparison, during the annealing process of 3Tm/2Cr/3Al/xO, a large portion of the octahedrally coordinated Cr(III) oxyhydroxides (40–50%) rearrange to tetrahedrally coordinated Cr(VI) early in the calcination process. This is followed by a reorganization to octahedrally coordinated Cr(III). In samples annealed up to temperatures near T_c, as well as in the C-TmCrAlG product, Cr(III) exhibits only octahedral coordination.

Acknowledgments

We thank the Hamburger Synchrotronstrahlungslabor HASYLAB, especially G. Materlik and R. Frahm, for alloting beam time at the EXAFS II station. We are grateful to D. v. Ahlften, P. Behrens, and K. Lochte for their support during beam time. This work was supported by the Bundesminister für Forschung und Technologie (Project 03-GulHAM-2).

References

1. TH. J. A. POPMA AND A. M. VAN DIEPEN, *AIP Conf. Proc.* **24,** 123 (1974).
2. T. MATSUZAWA, K. OKAMURA, T. SHISHIDO, AND S. YAJIMA, *J. Phys. (Paris)* **C2,** 149 (1979).
3. E. M. GYORGY, K. NASSAU, M. EIBSCHÜTZ, J. V. WASZCZAK, C. A. WANG, AND J. C. SHELTON, *J. Appl. Phys.* **50,** 2883 (1979).
4. F. J. LITTERST, J. TEJADA, AND G. M. KALVIUS, *J. Appl. Phys.* **50,** 7636 (1979).
5. N. SCHULTES, H. SCHIEDER, F. J. LITTERST, AND G. M. KALVIUS, *J. Magn. Magn. Mater.* **31–34,** 1507 (1983).
6. N. SCHULTES, Dissertation, Ludwig-Maximilians-Universität, Munich, FRG, 1984.
7. W. GIRNUS, H. BEUTHIEN, R. PRIESS, AND W. GUNSSER, *J. Magn. Magn. Mater.* **54–57,** 225 (1986).
8. G. WINKLER, "Magnetic Garnets", p. 25, Vieweg Verlag, Braunschweig (1981).
9. H. BEUTHIEN, A. TORKLER, W. GUNSSER, AND W. NIEMANN, *Ber. Bunsen-Ges. Phys. Chem.* **91,** 1296 (1987).
10. H. NIEMANN, Dissertation, Universität Hamburg, Hamburg, FRG, 1988.
11. W. MALZFELDT, W. NIEMANN, R. HAENSEL, AND P. RABE, *Nucl. Instr. Meth.* **208,** 359 (1983).
12. V. P. CHALYI, E. N. LUKACHINA, AND L. M. SIMONOVICH, *Izv. Akad. Nauk. SSSR Neorg. Mater.* **12,** 607 (1976).
13. L. A. REZNITSKII, S. E. FILIPPOVA, A. V. LEONOV, AND L. M. VITING, *Iz. Akad. Nauk. SSSR Neorg. Mater.* **21**(5), 744 (1985); **21**(6), 926 (1985).
14. P. A. LEE, P. H. CITRIN, P. EISENBERGER, AND B. M. KINCAID, *Rev. Mod. Phys.* **53,** 769 (1981).
15. W. NIEMANN, *Physica B* **158,** 279 (1989).
16. R. W. G. WYCKOFF, "Crystal Structures," Wiley, New York (1968).
17. A. F. WELLS, "Structural Inorganic Chemistry," Oxford University Press (1984).
18. R. E. NEWHAM AND Y. M. DE HAAN, *Z. Kristallogr.* **117,** 235 (1962).

19. J. S. Stephens and D. W. J. Cruickshank, *Acta Crystallogr. Sect. B* **26,** 222 (1970).
20. G. L. Glen and C. G. Dodd, *J. Appl. Phys.* **39,** 5372 (1966).
21. R. G. Shulman, Y. Yafet, P. Eisenberger, and W. E. Blumberg, *Proc. Natl. Acad. Sci. USA* **73,** 1384 (1976).
22. W. Niemann, B. S. Clausen, and H. Topsøe, *Catal. Lett.* **4,** 355 (1990).
23. G. Calas, J. Petiau, and A. Manceau, *J. Phys. (Paris),* **C8,** 813 (1986).
24. A. Torkler, H. Beuthien, W. Gunsser, W. Niemann, *Ber. Bunsen-Ges. Phys. Chem.* **91,** 1300 (1987).
25. F. Studer and A. Le Bail, *J. Phys. (Paris),* **C8,** 781 (1986).
26. S. Geller and M. A. Gilleo, *J. Phys. Chem. Solids,* **3,** 30 (1957).